'5

CONF-901194--15

DE91 010187

# Controller Design for a Force-Reflecting Teleoperator System with Kinematically Dissimilar Master and Slave*

J. F. Jansen, R. L. Kress, and S. M. Babcock
Oak Ridge National Laboratory†
Robotics & Process Systems Division
P. O. Box 2008
Oak Ridge, Tennessee 37831-6304

**Abstract** The purpose of this paper is to develop a controller for a force-reflecting teleoperator system having kinematically dissimilar master and slave. The controller is a stiffness controller for both the master and the slave. A mathematical problem associated with representing orientations using Euler angles is described, and Euler parameters are proposed as a solution. The basic properties of Euler parameters are presented, specifically those pertaining to stiffness control. The stiffness controller for both the master and the slave is formulated using Euler parameters to represent orientation and a Liapunov stability proof is presented for the controller. The master portion of the control scheme is implemented on a 6-degree-of-freedom master.

## Introduction and Objectives

In the late 1940s Goertz and his colleagues at Argonne National Laboratory developed one of the earliest recognizable mechanical master/slave manipulators without force reflection. Later, in the early 1950s Goertz and his colleagues developed an electric master/slave manipulator with force-reflecting capabilities in which each slave joint servo was tied directly to the master joint servo since both the master and slave were kinematically similar. The control structure for these manipulators was the classical position-position controller. A positional difference between the slave and the master is reflected back as a drive signal to the master to push the human operator away from the object. Goertz's work is summarized in the references **[Goertz,54]**. The position-position control scheme has been the basic controller for almost all master/slave manipulators used by industry up to the present. When the master and slave are not kinematically similar, the design of the controller is particularly difficult. Bejczy developed the first force-reflecting teleoperation with dissimilar kinematics **[Bejczy,81]**. Three major issues are associated with this control problem: (1) orientation representation, (2) accurate force-reflection, and (3) redundancy resolution. Only the first two objectives will be elaborated upon in this paper. A brief discussion pertaining to the third will be included.

Representing the orientation between the master and slave and using that information for force reflection is one of the more difficult problems in the control of any teleoperated system with kinematically dissimilar master and slave. One of the objectives of this paper is the incorporation of Euler parameters into the controller design.

---

*Research sponsored by Wright-Patterson Air Force Base.
†Operated by Martin Marietta Energy Systems, Inc., for the U.S. Department of Energy under contract DE-AC05-84OR21400.

Dissimilar kinematic designs make simple joint positional differences no longer adequate for a force-reflecting manipulator. To achieve accurate force-reflection, a type of stiffness controller will be designed for both the master and the slave. Based on using both the master and slave jacobians **[Miyazaki,86]** an accurate force-reflecting controller for kinematically dissimilar manipulators is proposed. Differences in the specification of stiffness when stiffness controllers are used for robotic operation and teleoperation will be pointed out.

When the slave has more than 6-DOF, redundancy resolution needs to be addressed. Primarily, the master manipulator will be addressed in this paper but a brief discussion of controller design for a redundant slave will be included. The results are applied to a specific 6-DOF master manipulator and a 7-DOF slave manipulator at the Oak Ridge National Laboratory (ORNL).

The paper is organized as follows. First we will introduce orientation representation using Euler parameters and present several sections describing the applicable properties of Euler parameters such as uniqueness, Euler parameter rates, and their relationship to rotational matrices. Next, the stiffness controller will be presented including the slave redundancy resolution. Liapunov stability for a passive system will be discussed. The controller is then applied to a commercially available 6-DOF force-reflecting master. Finally, the motivation for using Euler parameters and ways to properly set the controller gains are discussed and conclusions are drawn.

## Euler Parameters

**Difficulties with Euler angles.** Three variables are needed to represent orientation, implying that there is considerable redundancy in a rotational matrix composed of nine terms. Euler angles (which differ from Euler parameters) have difficulties when applied to teleoperated systems having a master dissimilar from the slave. These difficulties will be pointed out more clearly but can be summarized: (1) Euler angles introduce artificial singularities. (2) Euler angles are not a natural representation for force reflection.

It has been stated that Euler angular representations of orientation can fail because they can introduce artificial singularities. In control algorithms employing angular rates, the failure manifests itself as infinite joint rates. These algorithmic singularities cannot always be placed out of reach of the operator because of the large workspace volume. Consider defining the end-effector orientation using a Z-Y-Z Euler angle set, where the first rotation is about the nominal z-axis, the second rotation is about the new y-axis produced after the first rotation, and the final rotation is about the new z-axis produced after the first and second rotations. It is desired to produce an incremental rotation $\theta^\circ$ in the positive direction about the x-axis, as shown in Fig. 1. To produce this rotation, first rotate $90^\circ$ in the counterclockwise direction about the z-axis to produce the x'y'z' coordinate system, then rotate $\theta^\circ$ in the clockwise direction about the y'-axis to produce the x"y"z" coordinate system, and finally rotate $90^\circ$ in the clockwise direction about the z"-axis to produce the x'''y'''z''' coordinate system, which is the desired result. The velocity about the z- and z"-axes will be infinite even for infinitesimally small desired rotations because the change in angle about the z- and z"-axes is $90^\circ$, regardless of the size of the desired change $\theta^\circ$. This can be verified mathematically by determining the relationship between the Euler angle rates ($\hat{\dot{\alpha}}$) and the instantaneous angular velocities about the x-, y-, z-axes ($\hat{\omega}$) of Fig. 1. This relationship is derived in Fu **[Fu,87;p.235]**. As expected, the relationship between $\hat{\dot{\alpha}}$ and $\hat{\omega}$ has a cosec($\beta$) term, where $\beta$ is the pitch angle, indicating infinite velocities at orientations having zero $\beta$.[1]

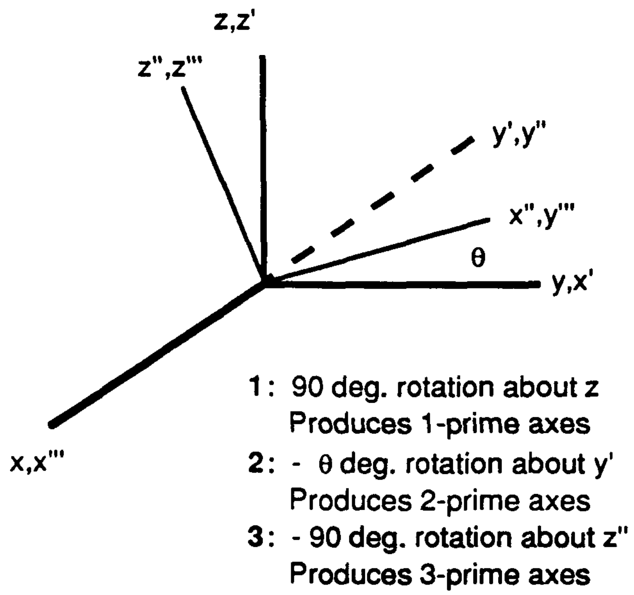


Fig. 1 Euler angle rotation about the x-axis.

Selection of another set of Euler angles only moves the singularity to another orientation. For example, consider using a yaw-pitch-roll set of Euler angles, where the first rotation is about the nominal (unrotated) x-axis, the second rotation is about the nominal (unrotated) y-axis, and the final rotation is about the nominal (unrotated) z-axis. The relationship between the Euler angle rates ($\hat{\dot{\alpha}}$) and the instantaneous angular velocities about the x-, y-, z-axes ($\hat{\omega}$) is derived in **[Fu,87;p.235]**. In this case, a sec($\beta$) term appears indicating infinite velocities at orientations having $\beta$ of $90^{\circ}$.

The conclusion from these observations has broad implications. For controllers using Euler angles to represent orientations with formulations requiring the relationship between the Euler angle rates ($\hat{\dot{\alpha}}$) and the instantaneous angular velocities about the x-, y-, z-axes ($\hat{\omega}$) to be known [e.g., resolved rate, stiffness (see Eq. 17) in this paper], artificial singularities will be introduced. These singularities may be moved to different locations in the manipulator work space by appropriate choice of Euler angle representations; however, they will never be eliminated completely. Clearly, another method of

---

[1] Unless otherwise stated, all variables with a cap ^ on top will denote a 3×1 vector in this paper.

representing orientations that does not produce these types of singularities is desirable.

**Euler parameters.** The notation followed in this paper is similar to Craig's notation **[Craig,89]**; the modifications for Paul's notation **[Paul,81]** will be clear from the context. Many of the matrix and vector relationships that are stated but not proven can be found in Yuan's work **[Yuan,88]** or at least in his references.

Let frame A, {A} and frame B, {B} be two arbitrary frames that are initially coincident. If {A} is fixed and {B} is rotated about a normalized vector ${}^{A}\hat{K}$ by an angle $\theta$ according to the right-hand rule, then the rotational matrix, ${}^{A}_{B}R$, relating a vector in {B} to {A} can be written in terms of ${}^{A}\hat{K}$ and $\theta$. The following Euler parameters are defined:

$$\varepsilon_1 = k_1 \sin\left(\theta/2\right) \quad , \tag{1}$$

$$\varepsilon_2 = k_2 \sin\left(\theta/2\right) \quad , \tag{2}$$

$$\varepsilon_3 = k_3 \sin\left(\theta/2\right) \quad , \tag{3}$$

$$\varepsilon_4 = \cos\left(\theta/2\right) \quad , \tag{4}$$

where ${}^{A}\hat{K} = [\, k_1 , k_2 , k_3 \,]^T$. Craig **[Craig,89;p.55]** shows that ${}^{A}_{B}R$ can be written as

$$ {}^{A}_{B}R = \begin{bmatrix} 1 - 2\varepsilon_2^2 - 2\,\varepsilon_3^2 & 2(\varepsilon_1\varepsilon_2 - \varepsilon_3\varepsilon_4) & 2(\varepsilon_1\varepsilon_3 + \varepsilon_2\varepsilon_4) \\ 2(\varepsilon_1\varepsilon_2 + \varepsilon_3\varepsilon_4) & 1 - 2\varepsilon_1^2 - 2\,\varepsilon_3^2 & 2(\varepsilon_2\varepsilon_3 - \varepsilon_1\varepsilon_4) \\ 2(\varepsilon_1\varepsilon_3 - \varepsilon_2\varepsilon_4) & 2(\varepsilon_2\varepsilon_3 + \varepsilon_1\varepsilon_4) & 1 - 2\varepsilon_1^2 - 2\,\varepsilon_2^2 \end{bmatrix} . \tag{5}$$

Because only three pieces of information are needed to adequately represent a rotational matrix, the Euler parameters satisfy the following additional constraint **[Yuan,88]**:

$$\varepsilon_1^2 + \varepsilon_2^2 + \varepsilon_3^2 + \varepsilon_4^2 = 1 \quad . \tag{6}$$

Let the first three Euler parameter terms be combined into a vector

$$\hat{\varepsilon} = \begin{bmatrix} \varepsilon_1 \\ \varepsilon_2 \\ \varepsilon_3 \end{bmatrix} \quad , \tag{7}$$

which is given with respect to {A} since ${}^{A}\hat{K}$ is given with respect to {A}. Equation (6) can be rewritten in vector notation as

$$\varepsilon_4^2 + \hat{\varepsilon}^T\hat{\varepsilon} = 1 \tag{8}$$

In this paper, the Euler parameters will be represented by the set $\{\varepsilon_4, \hat{\varepsilon}\}$.

**Uniqueness of representation of Euler parameter.** If the rotational angle $\theta$ is restricted between $-180 < \theta \leq 180$, then $\varepsilon_4$ is nonnegative and the Euler parameter representation is unique [**Yuan,88**]. Outside this range, the representation is not unique. By substitution into Eq. (5), both $\{\varepsilon_4, \hat{\varepsilon}\}$ and $\{-\varepsilon_4, -\hat{\varepsilon}\}$ can be shown to represent the same orientation. For teleoperation, restricting the range between $\pm$ 180 is adequate.

**Rotational matrix representation.** Equation (5) can be rewritten [**Yuan,88**] as

$$ {}^{A}_{B}R = \left(\varepsilon_4^2 - \hat{\varepsilon}^T\hat{\varepsilon}\right) I_3 + 2\,\hat{\varepsilon}\hat{\varepsilon}^T + 2\,\varepsilon_4\,\hat{\varepsilon}^{\times} \tag{9} $$

or

$$ {}^{B}_{A}R = \left(\varepsilon_4^2 - \hat{\varepsilon}^T\hat{\varepsilon}\right) I_3 + 2\,\hat{\varepsilon}\hat{\varepsilon}^T - 2\,\varepsilon_4\,\hat{\varepsilon}^{\times} = \left({}^{A}_{B}R\right)^T \quad , \tag{10} $$

where

$$ \hat{\varepsilon}^{\times} = \begin{bmatrix} 0 & -\varepsilon_3 & \varepsilon_2 \\ \varepsilon_3 & 0 & -\varepsilon_1 \\ -\varepsilon_2 & \varepsilon_1 & 0 \end{bmatrix} . \tag{11} $$

**Euler parameter rates.** Time derivatives of the Euler parameters will be used in the design of the stiffness controller. The Euler parameter rates can be written as

$$ \dot{\varepsilon}_4 = -\frac{1}{2}\hat{\varepsilon}^T\,\hat{\omega} \tag{12} $$

$$ \dot{\hat{\varepsilon}} = \frac{1}{2}\left(\varepsilon_4 I_3 - \hat{\varepsilon}^{\times}\right)\hat{\omega} \tag{13} $$

where $\hat{\omega}$ is the angular velocity vector with respect to $\{A\}$, and $\hat{\omega}^{\times}$ is defined the same as is $\hat{\varepsilon}^{\times}$ in Eq. (11). A slightly different formulation is given in Yuan [**Yuan,88**].

**Relative orientation.** The relative orientation between two rotational matrices can be defined in terms of the Euler parameters. Let ${}^{0}_{M}R$ and ${}^{0}_{S}R$ be two arbitrary matrices relating frames {M} and {S}, respectively, to the inertial frame {0}. The rotational matrix ${}^{M}_{S}R$ describing the orientational differences between these two frames is

$$ {}^{M}_{S}R = \left({}^{0}_{M}R\right)^T\,{}^{0}_{S}R \quad . \tag{14} $$

The Euler parameters of ${}^{M}_{S}R$, $\{\delta\varepsilon_4, \delta\hat{\varepsilon}\}$, can be written in terms of the Euler parameters of ${}^{0}_{M}R$ , $\{\varepsilon_M, \hat{\varepsilon}_M\}$, and ${}^{0}_{S}R$, $\{\varepsilon_S, \hat{\varepsilon}_S\}$ [**Yuan, 88**] as

$$ \delta\hat{\varepsilon} = \varepsilon_M\,\hat{\varepsilon}_S - \varepsilon_S\,\hat{\varepsilon}_M - \hat{\varepsilon}_M^{\times}\,\hat{\varepsilon}_S \tag{15} $$

and

$$\delta\varepsilon_4 = \varepsilon_M \varepsilon_S + \hat{\varepsilon}_M^T \hat{\varepsilon}_S \tag{16}$$

where $\delta\hat{\varepsilon}$ is with respect to {M}.

## Stiffness Controller Using Euler Parameters

**Master.** The master manipulator will incorporate a stiffness controller **[Salisbury,80]**. The torque signal is

$$\tau_m = J_m^T \{[K_{pm} (x_s - x_m) + K_{vm} (\dot{x}_s - \dot{x}_m)]\} + \tau_{m\,grav} \quad , \tag{17}$$

where the m subscript indicates master terms and

| | | |
|---|---|---|
| $J_m$ | = | master Jacobian, |
| $K_{pm}$ and $K_{vm}$ | = | positional and velocity gain matrices, respectively, |
| $\tau_{m\,grav}$ | = | torque signal to compensate for gravity effects, |
| $x_s$ and $\dot{x}_s$ | = | slave position and velocity, respectively, |
| $x_m$ and $\dot{x}_m$ | = | master position and velocity, respectively. |

For the Kraft manipulator (see "Application to the Kraft Master" section), counterbalance weights have been incorporated in its design making $\tau_{mgrav} \cong 0$. Typically, $K_{pm}$ and $K_{vm}$ are diagonal matrices

$$K_{pm} = \text{diag}(k_{pm}^1, \ldots, k_{pm}^6) \tag{18}$$

and

$$K_{vm} = \text{diag}(k_{vm}^1, \ldots, k_{vm}^6) \quad . \tag{19}$$

These matrices will be used in later derivations.

**Dynamics of a manipulator.** To understand the force reflection and transient response of the proposed controller, the dynamics of a manipulator in Cartesian space will be formulated. Assuming that the gravity component has already been compensated (i.e., by feedforward compensation), the dynamic equations of motion for all rigid-bodied link manipulators can be formulated **[Khatib,87]** as

$$M(q)\,\ddot{q} + C(q,\dot{q})\,\dot{q} + J(q)^T F_{ext} = \tau \quad , \tag{20}$$

where

$M(q) \quad \in R^{n \times n}$ is the inertia matrix,
$C(q,\dot{q}) \quad \in R^{n \times n}$ includes the Coriolis and centrifugal effects,
$J(q) \quad \in R^{6 \times n}$ is the manipulator Jacobian,
$F_{ext} \quad \in R^{6}$ is the contact force/torque vector,
$\tau \quad \in R^{n}$ is the joint torque vector,
$q \quad \in R^{n}$ is the generalized joint coordinates,
$n \quad =$ number of degrees of freedom (dof) of the manipulator.

For the rest of this paper the functional dependency of M, C, and J will be dropped to reduce notational clutter. Multiply Eq. (20) by $M^{-1}$ (since M is always nonsingular) to obtain the following:

$$\ddot{q} + M^{-1} C \dot{q} + M^{-1} J^T F_{ext} = M^{-1} \tau \quad . \tag{21}$$

Next, multiply Eq. (21) by J to obtain the following:

$$J \ddot{q} + J M^{-1} C \dot{q} + J M^{-1} J^T F_{ext} = J M^{-1} \tau \quad . \tag{22}$$

The definition of the manipulator Jacobian, J, is

$$\dot{x} = J \dot{q} \quad . \tag{23}$$

Taking the derivative of Eq. (23) with respect to time yields

$$J \ddot{q} = \ddot{x} - \dot{J} \dot{q} \quad . \tag{24}$$

Substitute Eq. (24) into Eq. (22) to obtain:

$$(\ddot{x} - \dot{J} \dot{q}) + J M^{-1} C \dot{q} + J M^{-1} J^T F_{ext} = J M^{-1} \tau \quad . \tag{25}$$

Define $M_x^{-1} = J M^{-1} J^T$ in Eq. (25) to produce

$$\ddot{x} + (J M^{-1} C - \dot{J}) \dot{q} + M_x^{-1} F_{ext} = J M^{-1} \tau$$

or

$$M_x \ddot{x} + M_x (J M^{-1} C - \dot{J}) \dot{q} + F_{ext} = M_x J M^{-1} \tau \quad . \tag{26}$$

Equation (26) is the general equation for manipulator dynamics in Cartesian coordinates.

**Slave controller and dynamics.** Now the results of the preceding section will be applied. The slave manipulator which is being considered in this paper has 7-DOF. The slave manipulator will incorporate a stiffness controller **[Salisbury,80 and Miyazaki,86]**. The torque signal is

$$\tau_s = J_s^T\left[K_{ps}\ (x_m - x_s) + K_{vs}\ (\dot{x}_m - \dot{x}_s)\right] + \tau_{s\,grav} + \tau_{red}\ , \tag{27}$$

where the s subscript indicates slave terms and

$J_s^T$ = transpose of the slave Jacobian,

$K_{ps}$ and $K_{vs}$ = positional and velocity gain matrices, respectively,

$\tau_{s\,grav}$ = torque signal to compensate for gravity,

$x_s$ and $\dot{x}_s$ = slave position and velocity, respectively,

$x_m$ and $\dot{x}_m$ = master position and velocity, respectively,

$\tau_{red}$ = redundancy torque.

The redundancy torque will be defined based on extended task-space techniques **[Oh,84 and Colbaugh,89]**. The basic idea is to add additional constraints to the system so that the end-effector jacobian is extended to have full rank. For the 7-DOF manipulator used in this research, adding a constraint to the elbow is convenient (other possibilities exist and will be addressed in a later paper), that is,

$$\tau_{red} = J_{red}^T\left[K_{pselb}\left(\hat{x}_{elb}^{des} - \hat{x}_{elb}\right)\right] - k_{damp}\,\dot{q}_s \tag{28}$$

where

$\dot{q}_s$ = slave joint velocity vector,

$\hat{x}_{elb}$ = elbow position in Cartesian position,

$\hat{x}_{elb}^{des}$ = desired elbow position in Cartesian position,

$k_{damp}$ = positive damping constant,

$K_{pselb}$ = positive semi-definite matrix,

$J_{red}$ = redundancy jacobian.

$J_{red}$ has the property that $J_{red}\dot{q}_s = \tilde{I}\,\dot{\hat{x}}_{elb}$, where $\tilde{I} = [I_3\ 0_3]^T$, $I_3 = 3\times3$ identity matrix and $0_3 = 3\times3$ zero matrix. More will be said about this controller in a later paper; however, a discussion concerning the stability of the master/slave system will be presented here.

Assume that feedforward compensation has been incorporated to make $\tau_{s\,grav} \cong 0$; consequently, for the rest of the discussion in this paper it will be set to zero. The redundancy torque, $\tau_{red}$, is used to exploit the redundancy of the extra DOF without resorting to pseudoinverse techniques.

Similar to the master, $K_{ps}$ and $K_{vs}$ are diagonal matrices

$$K_{ps} = \mathrm{diag}(k_{ps}^1, \ldots, k_{ps}^6) \tag{29}$$

and

$$K_{vs} = \mathrm{diag}(k_{vs}^1, \ldots, k_{vs}^6) \quad . \tag{30}$$

If, at steady state, the manipulator is stationary, then use of Eq. (26) will obtain the following result:

$$K_{ps}\,(x_s - x_m) + F_{sext} - \bar{J}^T \tau_{red} = 0 \quad , \tag{31}$$

where

$$\bar{J} = M^{-1} J^T \left(J\, M^{-1} J^T\right)^{-1} \tag{32}$$

or

$$\bar{J} = \left(M_x J M^{-1}\right)^T \quad . \tag{33}$$

$\bar{J}$ is the the generalized inverse that minimizes kinetic energy **[Whitney,72]**.

Equation (31) indicates that the stiffness of the end-effector depends only on the difference between the slave and master position and the redundancy torque. If $\bar{J}^T \tau_{red}$ is either small or zero, then the slave external force is proportional to the positional differences in Cartesian coordinates in steady state.

Equation (26) shows that coupling still exists between slave states because $M_x$ typically will not be a diagonal matrix. This indicates that the transient response of the end effector will be very complex. An eigenvalue analysis of the linearization in joint space of Eq. (20) using $\tau$ from Eq. (27) (assuming the manipulator is stationary and the $\tau_{red}$ and $\tau_{s\,grav}$ terms are zero) indicates that the eigenvalues will move significantly in the left half of the s-plane **[An,88]**. The linearized equation is

$$M_s\, \delta\ddot{q}_s + \left(J_s^T K_{vs} J_s + k_{damp} I_7\right) \delta\dot{q}_s + J_s^T K_{ps} J_s\, \delta q_s = 0 \quad , \tag{34}$$

where $I_7$ is a 7×7 identity matrix. The mean eigenvalue **[Asada,87]** is defined as

$$\sigma \equiv \frac{\sum_{i=1}^{2n} \lambda_i}{2n} = \frac{-\,\mathrm{Trace}\left(M_s^{-1} J_s^T K_{vs} J_s + k_{damp}\, M_s^{-1}\right)}{2n} \quad . \tag{35}$$

Physically, the mean eigenvalue provides a quantitative measure of the average damping of the system. The mean eigenvalue for stiffness control can vary significantly but usually has a value less than position-position control **[An,88]**.

The slave position, $x_s$, and the master position, $x_m$, of Eq. (17) must be expressed mathematically. Both $x_s$ and $x_m$ are vectors and have to be at least of dimension 6×1 because six pieces of information are required to specify the spatial location and orientation in three dimensional space. The first three terms of these vectors are the linear Cartesian position (i.e., the x, y, and z coordinates). In Eq. (17), replace the first three terms in $x_s - x_m$ with $\widehat{\Delta x}$. The first three terms in $\widehat{\Delta x}$ will be the linear Cartesian position difference between the slave and master with respect to the base frame. The next three variables in $x_s - x_m$, as proposed in this paper, should be the $\delta\hat{\varepsilon}$ vector addressed in the "Discussions Related to the Proposed Controller" section. It will be shown later that this scheme can be made stable and that no artificial singularities are introduced because of this angular formulation. Further, a physical argument to be presented later indicates that this scheme will give the human operator the "correct feel" required for force reflection by modifying the stiffness controller of the master and slave to include Euler parameters; that is,

$$\tau_m = J_m^T \left\{ K_{pm} \begin{bmatrix} \Delta\hat{x} \\ \delta\hat{\varepsilon} \end{bmatrix} + K_{vm} \begin{bmatrix} \Delta\dot{\hat{x}} \\ \delta\dot{\hat{\varepsilon}} \end{bmatrix} \right\} + \tau_{m\,grav} \quad , \tag{36a}$$

$$\tau_s = - J_s^T \left\{ K_{ps} \begin{bmatrix} \Delta\hat{x} \\ \delta\hat{\varepsilon} \end{bmatrix} + K_{vs} \begin{bmatrix} \Delta\dot{\hat{x}} \\ \delta\dot{\hat{\varepsilon}} \end{bmatrix} \right\} + \tau_{sgrav} + \tau_{red} \quad . \tag{36b}$$

Equation (6) is a constraining equation relating $\delta\hat{\varepsilon}$ to $\varepsilon_4$. Because of this constraint, only $\delta\hat{\varepsilon}$ is needed in the control algorithm (see **[Yuan,88]**). In the control algorithm, there are two Jacobians: the *master* Jacobian, $J_m$, and the *slave* Jacobian, $J_s$. These differ from the manipulator Jacobian (for an example, see [**Craig,89**]). The manipulator Jacobian is a transformation relating the joint rates to the Cartesian rates. The manipulator Jacobian for a 6-DOF manipulator is a 6×6 matrix whose $i^{th}$ column vector $j_i$ is given by Fu [**Fu,87**]:

$$j_i = \begin{cases} \begin{bmatrix} z_{i-1} \times {}^{i-1}p_6 \\ z_{i-1} \end{bmatrix} & \text{if joint i is rotational} \\ \begin{bmatrix} z_{i-1} \\ 0 \end{bmatrix} & \text{if joint i is translational} \end{cases} \quad , \tag{37}$$

where $z_{i-1}$ is the unit vector along the axis of motion of joint i expressed in the base coordinate frame and ${}^{i-1}p_6$ is the position of the origin of the hand coordinate frame from the origin of the $(i-1)^{st}$ coordinate frame, expressed in the base coordinate frame. The manipulator Jacobian of the master can be written as

$$J_{mf}\dot{q} = \begin{bmatrix} \dot{\hat{x}}_m \\ \hat{\omega}_m \end{bmatrix} , \qquad (38)$$

where $\dot{q}$ (6×1 vector) is the joint actuator rates and $\hat{\omega}$ is the angular velocity vector (3×1 vector) with respect to the base frame. The master and slave Jacobian is different from the manipulator Jacobian because the angular rates are based on Euler parameters. Define the (3×3) matrix W that relates the angular velocities $\hat{\omega}$ to $\dot{\delta\hat{\varepsilon}}$, that is,

$$\dot{\delta\hat{\varepsilon}} = W\,\hat{\omega} \ . \qquad (39)$$

The master Jacobian, $J_m$, is

$$J_m = \begin{bmatrix} I_3 & 0 \\ 0 & W \end{bmatrix} J_{mf} \ . \qquad (40)$$

Likewise, the slave Jacobian, $J_s$, and slave manipulator Jacobian, $J_{sf}$, can be defined similarly as

$$J_{sf}\dot{q} = \begin{bmatrix} \dot{\hat{x}}_s \\ \hat{\omega}_s \end{bmatrix} , \qquad (41a)$$

$$J_s = \begin{bmatrix} I_3 & 0 \\ 0 & W \end{bmatrix} J_{sf} \ . \qquad (41b)$$

To obtain the W matrix, first take the derivative of $\delta\hat{\varepsilon}$ in Eq. (15):

$$\dot{\delta\hat{\varepsilon}} = \dot{\varepsilon}_M \hat{\varepsilon}_S - \varepsilon_S \dot{\hat{\varepsilon}}_M - \dot{\hat{\varepsilon}}_M^{\times} \hat{\varepsilon}_S + \varepsilon_M \dot{\hat{\varepsilon}}_S - \dot{\varepsilon}_S \hat{\varepsilon}_M - \hat{\varepsilon}_M^{\times} \dot{\hat{\varepsilon}}_S \quad , \qquad (42)$$

which can be rewritten using Eqs. (12) and (13) as

$$\dot{\delta\hat{\varepsilon}} = W\left(\hat{\omega}_s - \hat{\omega}_m\right) \qquad (43)$$

where

$$W = 0.5\left[\hat{\varepsilon}_S \hat{\varepsilon}_M^{T} + \left(\varepsilon_S I_3 - \hat{\varepsilon}_S^{\times}\right)\left(\varepsilon_M I_3 - \hat{\varepsilon}_M^{\times}\right)\right] \ . \qquad (44)$$

Note that Eq. (43) is an exact representation relating Euler and angular rates. Small angle approximations used by other authors [Nguyen,90] have not been utilized in the derivation of Eq. (43). Using Eqs. (40) and (41b), Eqs. (38) and (41a) can be formulated into the more useful form that will be utilized in the Liapunov stability proof:

$$J_s \dot{q}_s - J_m \dot{q}_m = \begin{bmatrix} \dot{\hat{x}}_s - \dot{\hat{x}}_m \\ W(\hat{\omega}_s - \hat{\omega}_m) \end{bmatrix} = \begin{bmatrix} \Delta\dot{\hat{x}} \\ \dot{\delta\hat{\varepsilon}} \end{bmatrix} \quad . \tag{45}$$

Next, the stability properties will be examined.

## Liapunov Stability

**Stability model.** The human operator and the environment will be modeled as a spring/dashpot model. There are limitations with representing the operator and environment with passive models [**Anderson,89**]; nevertheless, investigations using a passive model build confidence with the proposed control techniques.

To show positional stability of stiffness control, a Liapunov function candidate is written as

$$L = 0.5\, \dot{q}_m^T M_m \dot{q}_m + 0.5\, \alpha\, \dot{q}_s^T M_s \dot{q}_s + 0.5\, (x_m - x_s)^T K_{p1} (x_m - x_s) + 0.5\, (x_{des} - x_m)^T K_{p2} (x_{des} - x_m) + 0.5\, \left(\hat{x}_{elb}^{des} - \hat{x}_{elb}\right)^T K_{elb} \left(\hat{x}_{elb}^{des} - \hat{x}_{elb}\right) \quad , \tag{46}$$

where

$x_{des}$ = position of the operator's hand (i.e., desired master position),

$K_{p1}$ , $K_{p2}$ , and $K_{elb}$ are > 0,

$\alpha$ is > 0.

The dynamic model for the master is

$$M_m \ddot{q}_m + C_m \dot{q}_m + \tau_{mgrav} + J_{mf}^T F_{hand} = \tau_m \quad , \tag{47}$$

where $F_{hand}$ is the force exerted by the operator's hand. The $F_{hand}$ term will be modeled as a spring with damping; that is,

$$F_{hand} = K_{phand} (x_m - x_{des}) + K_{vhand} \dot{x}_m \quad , \tag{48}$$

where $K_{phand}$ and $K_{vhand}$ are > 0.

The slave dynamic model is

$$M_s \ddot{q}_s + C_s \dot{q}_s + \tau_{sgrav} + J_{sf}^T F_{sext} = \tau_s \quad . \tag{49}$$

The Liapunov function, L, of Eq. (46) is a continuously differentiable positive definite function in terms of $\Delta x$ and $\dot{q}_s$. According to Liapunov's second method, one needs to show for global stability that

$$\frac{dL}{dt} = \dot{L} < 0 \tag{50}$$

for all nontrivial trajectories.

**Stability proof.** Taking the derivative of the Liapunov function candidate, Eq. (46), with respect to time, yields the following:

$$\dot{L} = \dot{q}_m^T M_m \ddot{q}_m + \alpha\, \dot{q}_s^T M_s \ddot{q}_s + 0.5\, \dot{q}_m^T \dot{M}_m \dot{q}_m + 0.5\, \alpha\, \dot{q}_s^T \dot{M}_s \dot{q}_s$$
$$+ (x_m - x_s)^T K_{p1} (\dot{x}_m - \dot{x}_s) - (x_{des} - x_m)^T K_{p2}\, \dot{x}_m - \left(\hat{x}_{elb}^{des} - \hat{x}_{elb}\right)^T K_{elb}\, \dot{\hat{x}}_{elb} \quad . \tag{51}$$

Using Eqs. (47) and (49), this derivative becomes

$$\dot{L} = \dot{q}_m^T \left( - C_m \dot{q}_m - \tau_{mgrav} - J_{mf}^T F_{hand} + \tau_m \right) + \alpha\, \dot{q}_s^T \left( - C_s \dot{q}_s - \tau_{sgrav} - J_{sf}^T F_{sext} + \tau_s \right)$$
$$+0.5\, \dot{q}_m^T \dot{M}_m \dot{q}_m + 0.5\, \alpha\, \dot{q}_s^T \dot{M}_s \dot{q}_s + (x_m - x_s)^T K_{p1} (\dot{x}_m - \dot{x}_s) - (x_{des} - x_m)^T K_{p2}\, \dot{x}_m$$
$$- \left(\hat{x}_{elb}^{des} - \hat{x}_{elb}\right)^T K_{elb}\, \dot{\hat{x}}_{elb} \quad . \tag{52}$$

Next, using Eqs. (17) and (27) and recalling that all gravity forces have been compensated, Eq. (52) becomes

$$\dot{L} = \dot{q}_m^T \left\{ - C_m \dot{q}_m - J_{mf}^T F_{hand} + J_m^T \left[ K_{pm} (x_s - x_m) + K_{vm} (\dot{x}_s - \dot{x}_m) \right] \right\}$$
$$+ \alpha\, \dot{q}_s^T \left\{ - C_s \dot{q}_s - J_{sf}^T F_{sext} + J_s^T \left[ K_{ps} (x_m - x_s) + K_{vs} (\dot{x}_m - \dot{x}_s) \right] + \tau_{red} \right\}$$
$$+0.5\, \dot{q}_m^T \dot{M}_m \dot{q}_m + 0.5\, \alpha\, \dot{q}_s^T \dot{M}_s \dot{q}_s + (x_m - x_s)^T K_{p1} (\dot{x}_m - \dot{x}_s) - (x_{des} - x_m)^T K_{p2}\, \dot{x}_m$$
$$- \left(\hat{x}_{elb}^{des} - \hat{x}_{elb}\right)^T K_{elb}\, \dot{\hat{x}}_{elb} \quad . \tag{53}$$

Using the matrix relationships **[Asada,86;p.137]**:

$$\dot{M}_m - 2\, C_m = 0 \tag{54a}$$

and

$$\dot{M}_s - 2\, C_s = 0 \tag{54b}$$

in Eq. (53) results in

$$\dot{L} = \dot{q}_m^T \left\{ - J_{mf}^T F_{hand} + J_m^T \left[ K_{pm} (x_s - x_m) + K_{vm} (\dot{x}_s - \dot{x}_m) \right] \right\}$$
$$+ \alpha\, \dot{q}_s^T \left\{ - J_{sf}^T F_{sext} + J_s^T \left[ K_{ps} (x_m - x_s) + K_{vs} (\dot{x}_m - \dot{x}_s) \right] + \tau_{red} \right\}$$
$$+ (x_m - x_s)^T K_{p1} (\dot{x}_m - \dot{x}_s) - (x_{des} - x_m)^T K_{p2}\, \dot{x}_m - \left(\hat{x}_{elb}^{des} - \hat{x}_{elb}\right)^T K_{elb}\, \dot{\hat{x}}_{elb} \quad . \tag{55}$$

Let $K_{pm} = \alpha\, K_{ps}$ and $K_{vm} = \alpha\, K_{vs}$, which means that the slave and master gains are related by an arbitrary positive constant and that $K_{pl} = K_{pm} = \alpha K_{ps}$. Using the definition of the master and slave Jacobians given in Eqs. (38) and (41) and recognizing that $\dot{x} = J\dot{q}$ yields $\dot{x}^T = \dot{q}^T J^T$ Eq. (55) can be further simplified to:

$$\dot{L} = \dot{q}_m^T \left( - J_{mf}^T F_{hand} \right) + \alpha\, \dot{q}_s^T \left( - J_{sf}^T F_{sext} + \tau_{red} \right)$$
$$- (\dot{x}_m - \dot{x}_s)^T K_{vm} (\dot{x}_m - \dot{x}_s) - (x_{des} - x_m)^T K_{p2}\, \dot{x}_m - \left(\hat{x}_{elb}^{des} - \hat{x}_{elb}\right)^T K_{elb}\, \dot{\hat{x}}_{elb} \quad . \tag{56}$$

Examine Eq. (56) under the following cases:

Case 1: Set $F_{sext} = 0$. This condition implies that the slave is moving in free space. Using Eq. (48), Eq. (56) reduces to

$$\dot{L} = \dot{q}_m^T \left\{ - J_{mf}^T \left[ K_{phand} (x_m - x_{des}) + K_{vhand}\, \dot{x}_m \right] \right\} + \alpha\, \dot{q}_s^T \tau_{red}$$

$$- (\dot{x}_m - \dot{x}_s)^T K_{vm} (\dot{x}_m - \dot{x}_s) - (x_{des} - x_m)^T K_{p2} \dot{x}_m - \left(\hat{x}_{elb}^{des} - \hat{x}_{elb}\right)^T K_{elb} \dot{\hat{x}}_{elb} \quad . \qquad (57)$$

Set $K_{p2} = K_{phand}$ and recall the definition of the master manipulator Jacobian given in Eq. (38). Eq. (57) reduces to:

$$\dot{L} = - \dot{x}_m^T K_{vhand} \dot{x}_m - (\dot{x}_s - \dot{x}_m)^T K_{vm} (\dot{x}_s - \dot{x}_m) - \left(\hat{x}_{elb}^{des} - \hat{x}_{elb}\right)^T K_{elb} \dot{\hat{x}}_{elb} + \alpha \dot{q}_s^T \tau_{red} \, . \qquad (58)$$

Set $K_{elb} = \alpha K_{pselb}$ and use the definition of $\tau_{red}$ from Eq. (28) to reduce Eq. (58) to

$$\dot{L} = - \dot{x}_m^T K_{vhand} \dot{x}_m - (\dot{x}_s - \dot{x}_m)^T K_{vm} (\dot{x}_s - \dot{x}_m) - \alpha k_{damp} \dot{q}_s^T \dot{q}_s \quad . \qquad (59)$$

Eq. (59) shows that $\dot{L}$ is negative semi-definite. By LaSalle's Theorem [**Miyazaki,86**], asymptotic stability is shown.

Case 2: Set $F_{sext} = K_{psext} (x_s - x_E) + K_{vsext} \dot{x}_s$, which is the case when the slave touches the environment at $x_E$. Augment the Liapunov function in Eq. (46) with an additional term:

$$L \rightarrow L + 0.5(x_s - x_E)^T K_{p3} (x_s - x_E) \quad , \qquad (60)$$

where $K_{p3}$ is a positive definite matrix. With $K_{p2} = K_{phand}$ and noting that $\dot{x}_E = 0$, $\dot{L}$ is written as

$$\dot{L} = \dot{q}_m^T\left( - J_{mf}^T K_{vhand} \dot{x}_m + \nu J_{mf} F_s\right) - \alpha \dot{q}_s^T \left( J_{sf}^T K_{psext} (x_s - x_E) + J_{sf}^T K_{vsext} \dot{x}_s \right)$$
$$- (\dot{x}_m - \dot{x}_s)^T K_{vm} (\dot{x}_m - \dot{x}_s) + (\dot{x}_s)^T K_{p3} (x_s - x_E) - \alpha k_{damp} \dot{q}_s^T \dot{q}_s \quad . \qquad (61)$$

Let $K_{p3} = \alpha K_{psext}$ and use the definitions of the master and slave manipulator Jacobians. Eq. (61) becomes

$$\dot{L} = \dot{q}_m^T\left( - J_{mf}^T K_{vhand} \dot{x}_m \right) - \alpha \dot{q}_s^T \left( J_{sf}^T K_{vsext} \dot{x}_s \right) - (\dot{x}_m - \dot{x}_s)^T K_{vm} (\dot{x}_m - \dot{x}_s) - \alpha k_{damp} \dot{q}_s^T \dot{q}_s \qquad (62)$$

or

$$\dot{L} = \left( - \dot{x}_m^T K_{vhand} \dot{x}_m \right) - \alpha \left( \dot{x}_s^T K_{vsext} \dot{x}_s \right) - (\dot{x}_m - \dot{x}_s)^T K_{vm} (\dot{x}_m - \dot{x}_s) - \alpha k_{damp} \dot{q}_s^T \dot{q}_s \qquad (63)$$

Eq. (63) shows that $\dot{L}$ is negative semi-definite. Again by LaSalle's Theorem, asymptotic stability is shown.

## Application to the Kraft Master

**Hardware.** The controller was implemented on the Kraft master controller, shown schematically in Fig. 2. The Kraft KMC 9100-MC is a lightweight 6-DOF master arm designed, manufactured, and sold by Kraft Telerobotics, Inc., of Overland Park, Kansas. Position is measured at each joint by potentiometers. The first five joints are actuated by ac servomotors for

Denavit-Hartenberg Table

| $q_i$ (deg) | $d_i$ (m) | $a_{i-1}$ (deg) | $a_{i-1}$ (m) | $q$ (deg) |
|---|---|---|---|---|
| $q_1$ | 0 | 0 | 0 | 0 |
| $q_2$ | $d_2$ | 90 | 0 | +90 |
| $q_3$ | 0 | 0 | $a_2$ | -90 |
| $q_4$ | $d_4$ | -90 | $a_3$ | 0 |
| $q_5$ | 0 | 90 | 0 | +90 |
| $q_6$ | $d_6$ | 90 | 0 | 0 |

Note: $d_2$ = 0.073 m, $d_4$ = 0.084 m, $d_6$ = 0.114 m
$a_2$ = 0.178 m, $a_3$ = 0.203 m

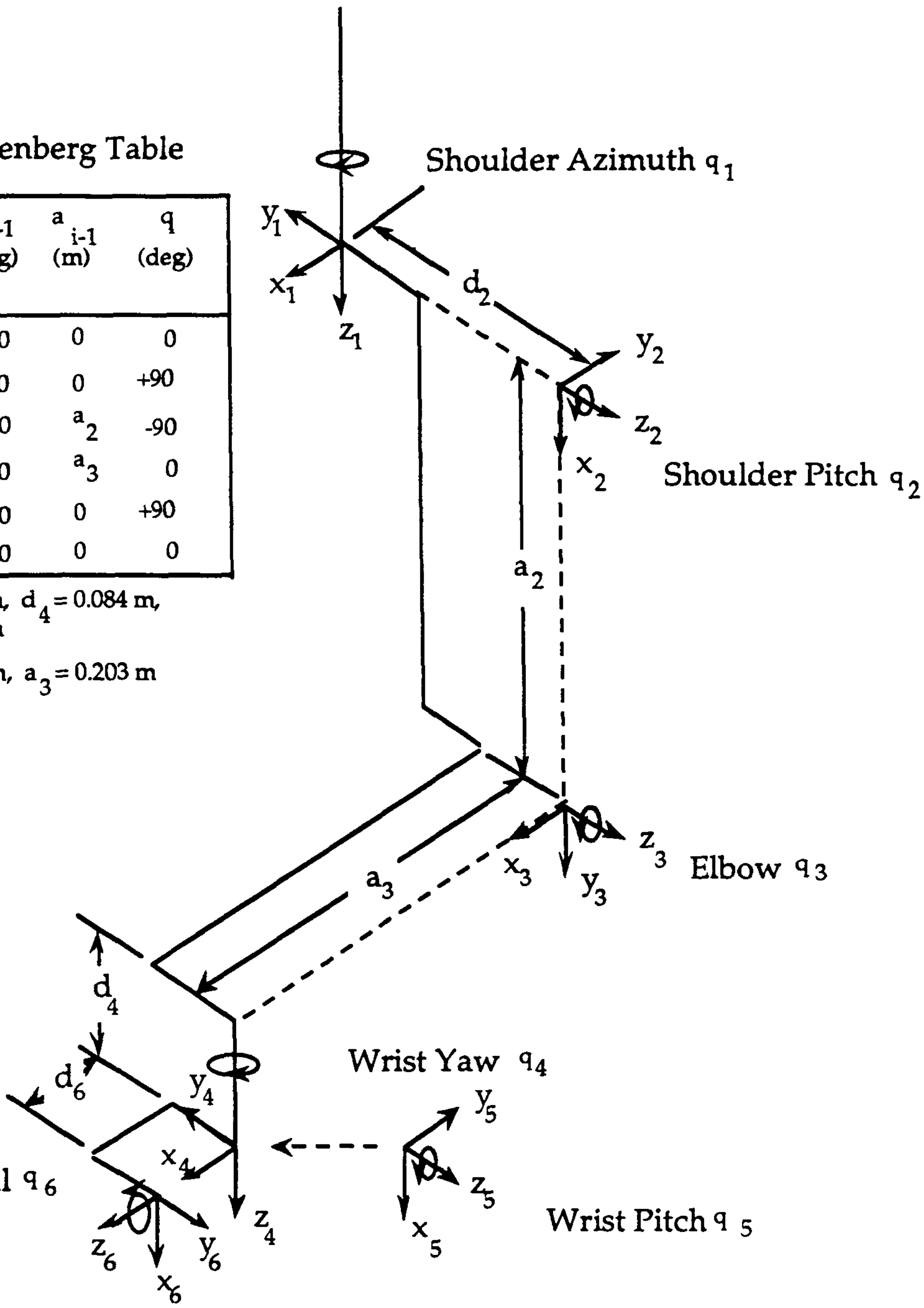


Fig. 2 Kinematic diagram and Denavit-Hartenberg table for the Kraft master manipulator.

force feedback. Wrist roll is not actuated. The Kraft arm is sold with the KMC 9100S electronics interface unit. Kress **[Kress,90]** has further details.

**Implementation.** In some ways, this section is the salient feature of the paper. The control algorithm was programmed in the C language on a Motorola 68020 with a 68881 floating-point coprocessor. The control algorithm was optimized by (1) factoring the Jacobians (see the appendix) so that common terms were not recalculated and (2) using a special assembly language routine that simultaneously determines the sine and cosine of each joint angle. When implemented, the master code ran at ~60 Hz, including the communication overhead.

Torque vs applied signal was measured in the laboratory for each of the five actuated joints on the Kraft master. A plot of the torque vs applied signal for each joint of the Kraft manipulator is shown in Fig. 3.

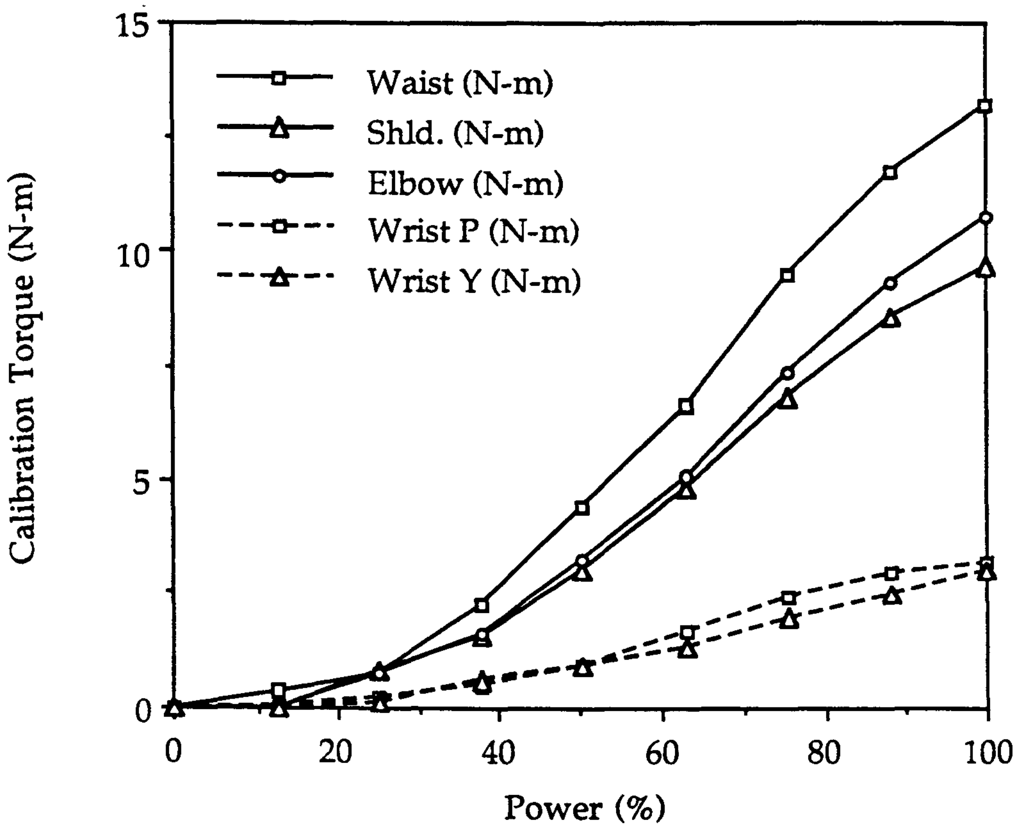


Fig. 3 Response of Kraft manipulator joints.

Figure 3 shows ~10% deadband in each joint. Some compensation is required to optimize between good backdrivability and force sensitivity when using a master with these levels of deadband. For a master having friction that consists mainly of stiction and coulomb friction, a simple form of compensation is an offset function, called the preload function (PLF), which is the inverse of a deadband function [Gelb, 68]. The PLF function is shown in Fig. 4.

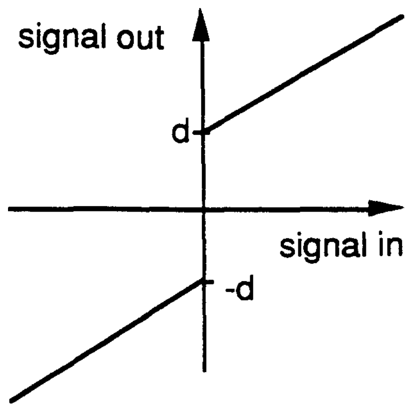


Fig. 4 Preload function for friction compensation.

An analysis was performed using describing function methods to determine whether limit cycles would be present when applying the preload function. A limit cycle is defined to be an initial condition-independent periodic oscillation occurring in dissipative systems **[Gelb,68]**. Figure 5 shows a block diagram of a single joint controller for the master. The following definitions are helpful:

1. NLF is the nonlinear friction block comprising coulomb friction and stiction (N-m).
2. Kp and Kv represent position and velocity gains.
3. KT is the motor torque constant (N-m/A).
4. $J_L$ is the load inertia (kg-m$^2$).
5. Kvf represents viscous damping (N-m/rad/s).
6. PLF is the preload function (A/rad).
7. $\theta_{des}$ is the desired joint angle (rad).
8. $\theta_L$ and $\dot{\theta}_L$ are the output (load) angle (rad) and angular velocity (rad/s), respectively.
9. 1/s indicates integration.

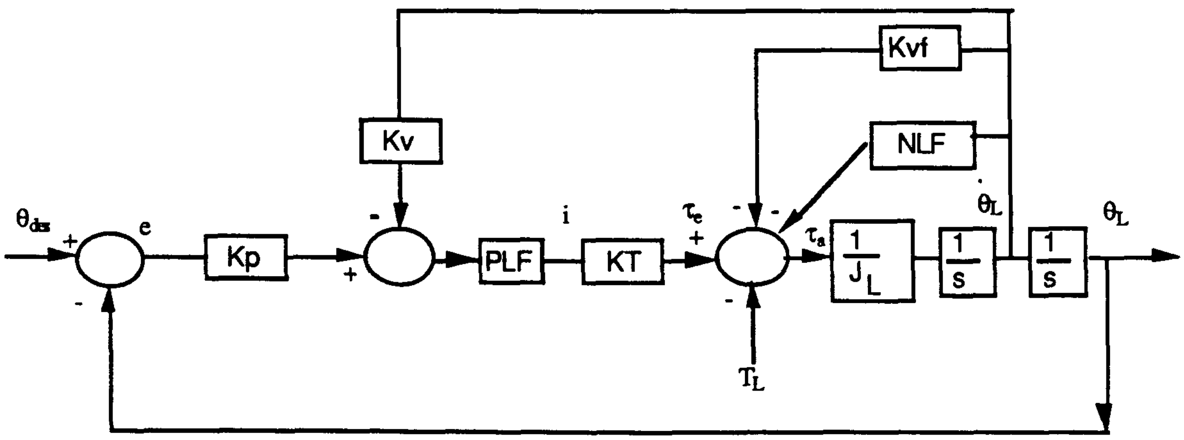


Fig. 5 Block diagram of a single master joint.

Making the assumptions that the filter hypothesis holds and sinusoidal waveforms are present, set $\theta_L = A \sin \omega t$ [**Gelb,68**]. Setting the input and load torque to zero, the following equations must be satisfied for a limit cycle to exist:

$$A\,(K_{vf} + KT\,K_v) + A\,n_{NLF} = 0 \tag{64}$$

and

$$K_pKT\,(A/\omega)\,n_{PLF} = A\,J_L\,\omega \tag{65}$$

where $n_{PLF}$ is the describing function for the PLF block and $n_{NLF}$ is the describing function for the nonlinear friction block. Since $n_{PLF}$ and $n_{NLF}$ are both real positive functions, the only solution to Eqs. (66) and (67) is A = 0 and $\omega$ = arbitrary; therefore, a limit cycle will not occur [**Gelb,68**]. If, however, there are significant amounts of backlash (not modeled in Fig. 5), then a limit cycle might occur. This was not true when the controller was implemented on the Kraft master arm.

The PLF was implemented on the master controller. For most of the joints, the preload was set to ~10% except for the wrist pitch and yaw. For these joints, the preload was reduced to ~5% to avoid a chattering at the switching line between plus and minus preload. The PLF did not introduce any instabilities, and it improved the force reflection.

Figures 6a and 6b show the high-level block diagrams of both the master and slave controller, respectively.

**MASTER CONTROLLER**

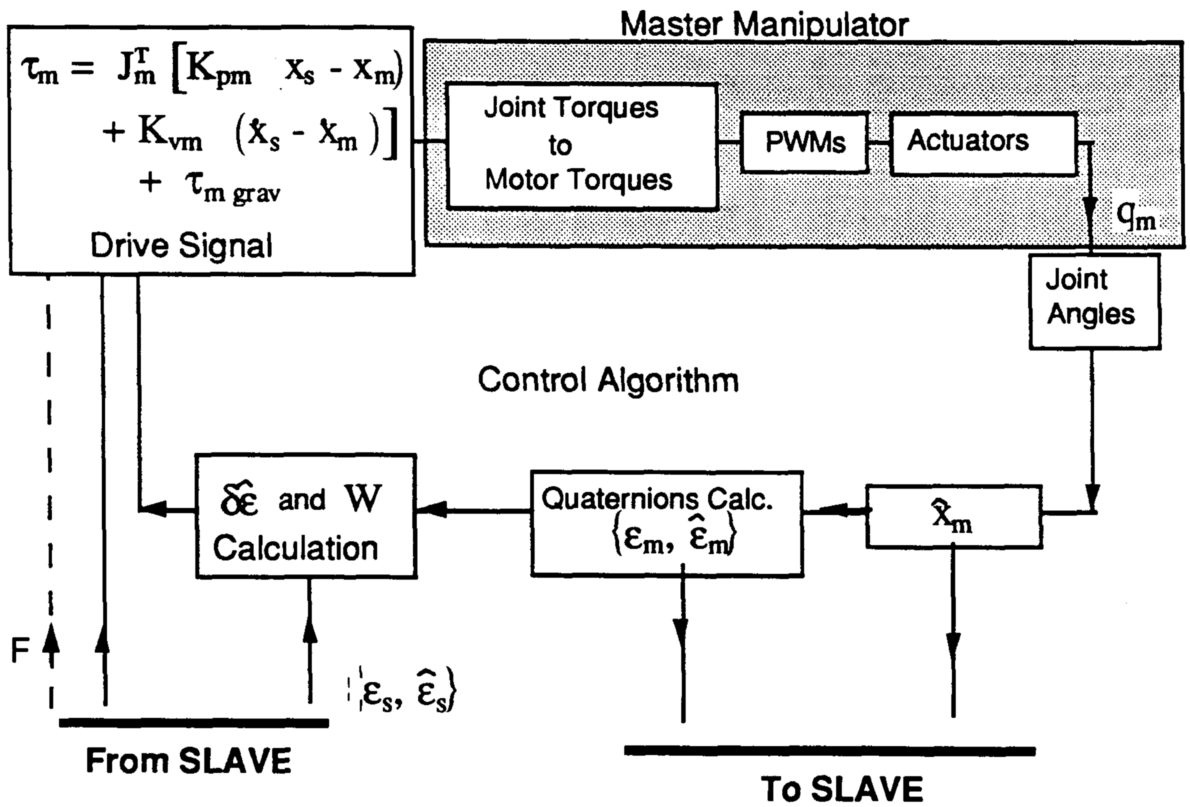


Fig. 6a Master Controller

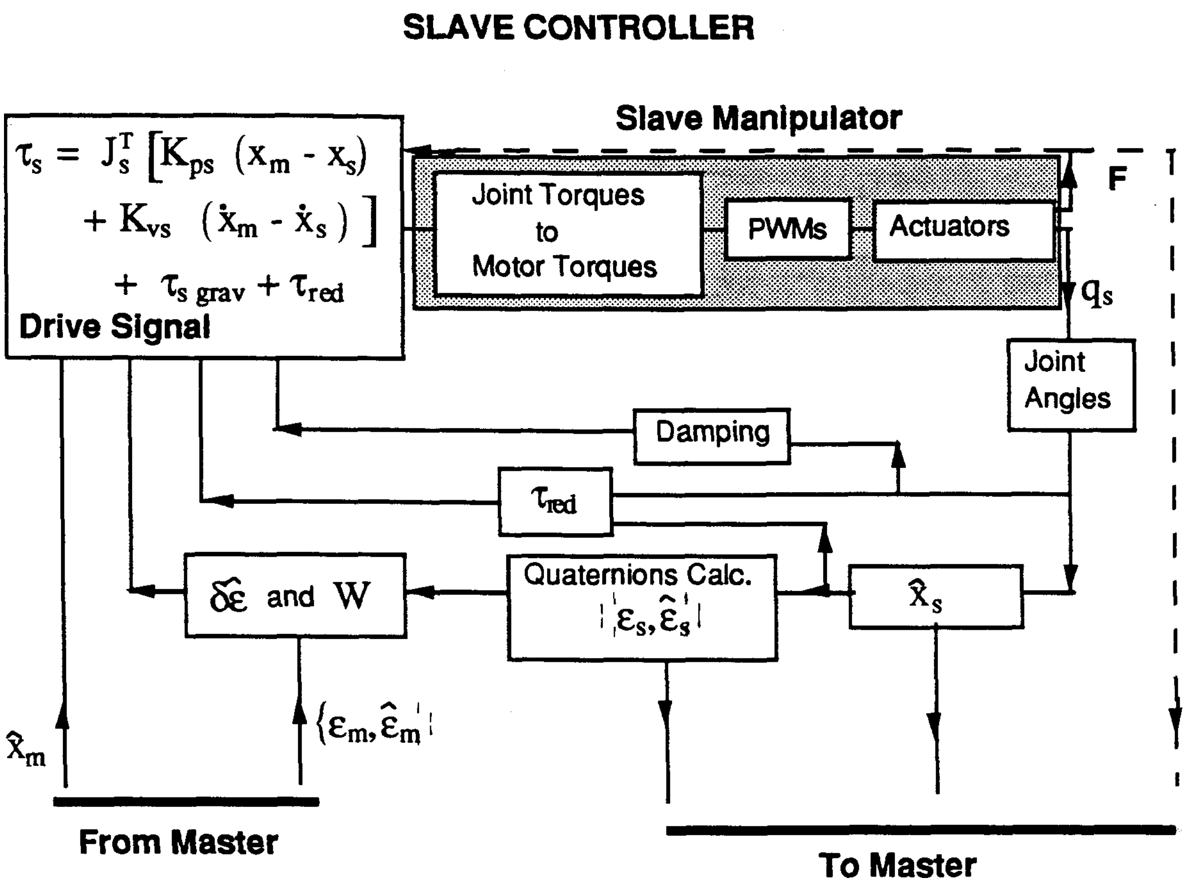


Fig. 6b Slave Controller

The dashed line represents a force/torque signal from the JR3 sensor and will be discussed in the conclusion. The computational requirements are modest. A single MC 68020 with a math coprocessor can easily perform the computational requirements for each controller.

## Discussions Related to the Proposed Controller

**Motivation for Using Euler Parameter.** It has been shown that the stiffness controller based on Euler parameters does not introduce artificial singularity points and that stability is guaranteed, assuming passive models. The purpose of this section is to motivate the use of Euler parameters to represent orientation.

Angular positional differences for large displacements are not vector quantities; therefore, the expression

$$\int \hat{\omega}_m dt - \int \hat{\omega}_s dt \qquad (66)$$

has no meaning as a vector difference for large positional differences because components cannot be subtracted, **[Asada,86 and Yuan,88]**. This is a fundamental difference between linear Cartesian differences and angular differences. Euler parameters provide a means for defining an angular difference in terms of the $\hat{\delta\varepsilon}$ vector. If $\tilde{\omega}$ is defined as the product of the (3×3) matrix W of Eq. (44) and $\hat{\omega}$, then the expression

$$\int \tilde{\omega}_m dt - \int \tilde{\omega}_s dt = \int (\tilde{\omega}_m - \tilde{\omega}_s) dt \qquad (67)$$

has meaning as a vector difference.

Further, the magnitude (Euclidean norm) of $\hat{\delta\varepsilon}$ is proportional to the sine of the half-angular difference between frames, as can be seen in Eqs. (1) through (3). For small angular displacements, $\hat{\delta\varepsilon}$ is proportional to the angular difference between frames, which is the feel an operator desires. As the angular displacements increase, the sine function will act as a saturation function, preventing the feedback of excessive forces. Large angular displacements are possible on systems (most working systems have bandwidths under 3 Hz.) that have appreciable tracking phase lag between master and slave.

**Gain Selection for the Stiffness Controllers.** While both the master and the slave incorporate a stiffness controller, the requirements are different for robotic operation. For robotic stiffness control, the interaction between the environment and the robot arm is specified [**An,88**]. For teleoperation, the purpose is to reflect the environmental forces and stiffness accurately to the human operator. The human operator will vary impedance according to changes in the slave impedance [**Hogan,85**]. To achieve this, the positional gain matrices for both the master and slave, $K_{pm}$, and, $K_{ps}$, are adjusted so that they are made large but not so large as to produce limit cycles [**Gelb,68**].

A dichotomy exists when tuning a stiffness controller for a teleoperator system. For an ideal teleoperator, the slave joint position should track the master position and likewise the slave forces on its end-effector should track the master forces on its end-effector. The mechanical equivalent indicates that the master and slave should be tightly coupled and there should be zero compliance between the two (or an infinite stiffness coupling the two). At steady state, the operator stiffness will be reflected to the slave as shown in Fig. 7, where the operator is simply modeled as passive spring with stiffness $K_{oper}$, and the teleoperator stiffness is $K_p$.

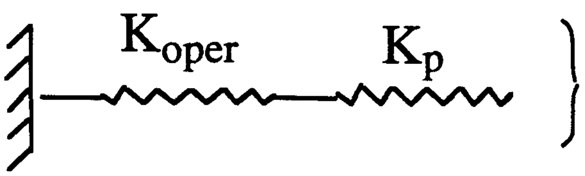


$$K_{eq} = \frac{1}{\frac{1}{K_{oper}} + \frac{1}{K_p}}$$

Fig. 7 Operator stiffness reflected to slave.

The equivalent stiffness $K_{eq}$ will in the limit approach $K_{oper}$ when $K_p$ approaches infinity. Since infinite stiffness is not physically achievable, $K_p$

should be set to as large a value as possible while avoiding limit cycles. Compensators can be designed to allow large values of $K_p$ while avoiding limit cycles (details can be found in **[Jansen,90]**).

## Conclusion

This paper has presented a formulation of a controller for a teleoperator system with dissimilar kinematics and force feedback. The controller is a stiffness controller for both the master and the slave. A mathematical problem associated with representing orientations using Euler angles has been described, and Euler parameters are proposed as an alternative. Euler parameters are superior to Euler angles not only because they do not introduce artificial singularities but also because they are a natural representation for force reflection. The basic properties of Euler parameters have been presented, specifically those pertaining to stiffness control. The stiffness controller for both the master and the slave has been formulated using the Euler parameters to represent orientation. A Liapunov stability proof is presented for the controller. Asymptotic stability is shown for two cases, namely, the slave moving in free space and the slave in contact with the environment.

The master controller is presently implemented on a 6-DOF, force-reflecting Kraft master manipulator and runs at a loop rate of ~60 Hz. The stiffness controller has worked well on the Kraft master manipulator. With the Euler parameter formulation, no artificial singularities are present as with the Euler angle formulation. Further, the magnitude (Euclidean norm) of $\delta\hat{\varepsilon}$ is proportional to the sine of the half angular difference between frames as can be seen in Eqs. (1) through (3). For small angular displacements, $\delta\hat{\varepsilon}$ is proportional to the angular difference between frames, which is the feel an operator desires. As the angular displacements increase, the sine function will act as a saturation function, preventing the feedback of excessive forces.

Force-reflection capability is enhanced by means of a force/torque sensor on the slave. This signal is sent back to the master after suitable transformations are made. Unfortunately for large force feedback gains, instabilities have been observed due to noncolocation of this sensor and phase-lag between master and slave.

The control algorithm can be extended using the manipulator Jacobian and artificial potential functions to create artificial walls and surfaces defined in Cartesian space to restrict operation in "forbidden zones." With proper gain settings, these surfaces can be given a "repelling" feel such that the operator must exert a strong force to pass through the surface. Dangerous obstacles (e.g., avoiding contact with the robot base) can be defined in the master's Cartesian space such that the operator cannot move the master to a location that would drive the slave into the obstacle.

## Appendix - Kraft Jacobian

The master Jacobian, ${}^3J$, has been symbolically determined in the third frame and checked by MACSYMA™ **[Symbolics,85]**. Note that the third frame is a convenient frame in which to formulate the Jacobian because, overall, the terms are in their simplest form. For example, determining the Jacobian in the final (hand) frame would simplify the lower right (3×3) block; however, the upper left (3×3) block would then be more complicated. Determining the Jacobian in a frame preceding a spherical wrist seems to produce the simplest form:

$$
{}^{3}J = \begin{bmatrix}
c_{23}(d_2 - s_4 s_5 d_6) & -d_4 + s_3 a_2 + c_5 d_6 & c_5 d_6 - d_4 & -s_4 s_5 d_6 & c_4 c_5 d_6 & 0 \\
s_{23}(c_3 s_4 s_5 d_6 - d_2) & a_3 + c_3 a_2 + c_4 s_5 d_6 & a_3 + c_4 s_5 d_6 & 0 & s_5 d_6 & 0 \\
s_{23}(d_4 - c_5 d_6) - c_{23}(a_3 + c_4 s_5 d_6) - c_2 a_2 & 0 & 0 & -c_4 s_5 d_6 & -s_4 c_5 d_6 & 0 \\
s_{23} & 0 & 0 & 0 & s_4 & c_4 s_5 \\
c_{23} & 0 & 0 & 1 & 0 & -c_5 \\
0 & 1 & 1 & 0 & c_4 & -s_4 s_5
\end{bmatrix} . \qquad \text{(A1)}
$$

## References


**[An,88]** An, C. H., Atkeson, C. G., and Hollerbach, J. M., Model-Based Control of a Robotic Manipulator, MIT Press, Cambridge, Massachusetts, 1988.

**[Anderson,89]** Anderson, R. and Spong, M., "Asymptotic Stability for Force Reflecting Teleoperators with Time Delay," *1989 IEEE International Conference on Robotics and Automation*, Vol. 3, May 1990, pp. 1618-1625.

**[Asada,86]** Asada, H. and Slotine, J.-J.. E., Robot Analysis and Control, John Wiley and Sons, New York, N. Y., 1986.

**[Asada,87]** Asada, H. and Youcef-Toumi, K., Direct-Drive Robots, MIT Press, Cambridge, Massachusetts, 1987.

**[Bejczy, 81]** Bejczy, A. K., and Handlykken, M., "Experimental Results with a Six-Degree-of-Freedom Force Reflecting Hand Controller," *Proceedings of the 17th Annual Conference on Manual Control*, UCLA, Los Angeles, California, June 16-18, 1981.

**[Colbaugh,89]** Colbaugh, R., Seraji, H., and Glass K. L., "Obstacle Avoidance for Redundant Robots Using Configuration Control," *J. of Robotic Systems*, Vol. 6, No. 6, pp.721-744, 1989.

**[Craig,89]** Craig, J. J., Introduction to Robotics: Mechanics and Control, Addison-Wesley, Reading, Mass. 1989.

**[Fu,87]** Fu, K. S., Gonzalez, R. C., and Lee, C. S. G., Robotics: Control, Sensing, Vision, and Intelligence, McGraw-Hill, Inc., New York, N. Y., 1987.

**[Gelb,68]** Gelb, A and Velde, W. E. V, Multiple-Input Describing Functions and Nonlinear System Design, McGraw-Hill, Inc., New York, N. Y., 1968.

**[Goertz,54]** Goertz, R. C. and Thompson, W. M., "Electronically Controlled Manipulator," *Nucleonics*, Nov. 1954, pp.46-47.

**[Hogan,85]** Hogan, N., "Impedance Control: An Approach to Manipulation: Part 1 - 3 Theory," *J. of Dynamic Systems, Measurement, and Control*, Vol. 107, March 1985, pp. 1-24.

**[Jansen,90]** Jansen, J. F. and J. N. Herndon, "Design of a Telerobotic Controller with Joint Torque Sensors," *1990 IEEE Internat. Conf. Robotics and Automation*, Vol. 2, May 1990, pp. 1109-1115 .

**[Khatib,87]** Khatib, O, "A Unified Approach for Motion and Force Control of Robot Manipulators: The Operational Space Formulation," *IEEE J. of Robotics and Automation*, Vol. RA-3, No. 1, Feb. 1987, pp. 43-53.

**[Kress,90]** Kress, R. L., Jansen, J. F., DePiero, F. W., and Babcock, S. M., " Force-Reflecting Control of a Teleoperator System Coupling a Nonredundant Master with a Redundant Slave," *Third International Symposium on Robotics and Manufacturing*, Vancouver, B.C., Canada, July 18-20, 1990.

**[Miyazaki,86]** Miyazaki, F., Matsubayashi, S., Yoshimi, T. and Arimoto, S., " A New Control Methodology Toward Advanced Teleoperation of Master-Slave Robot Systems," *1986 IEEE International Conference on Robotics and Automation*, Vol. 2, April 1986, pp. 997-1002.

**[Nguyen,90]** Nguyen, C. C., Zhou, Z. L., and Mosier, G. E., "Kinematic Analysis and Control of a 7-DOF Redundant Telerobot Manipulator," *Proc. of 22nd Southeastern Symposium on System Theory*, Cookeville, Tennessee, March 11-13, 1990, pp. 71-77.

**[Oh,84]** Oh, S. Y., D. Orin, and M. Bach., "An inverse Kinematic solution for kinematically redundant Robot Manipulators," *J. of Robotic Systems*, 1, pp. 235-249, 1984.

**[Paul,81]** Paul, R. P., Robot Manipulators: Mathematics, Programming, and Control. MIT Press, Cambridge, Mass. 1981.

**[Salisbury,80]** Salisbury, J. K., "Active Stiffness Control of a Manipulator in Cartesian Coordinates," IEEE Conf. Decision and Control, Albuquerque, New Mexico, Nov. 1980, pp. 95-100.

**[Symbolics,85]** MACSYMA, Reference Manual Version 11, Symbolics Inc., 1985.

**[Whitney,72]** Whitney, D. E., "The Mathematics of Coordinated Control of Prosthetic Arms and Manipulators," *ASME J. of Dynamic Systems Measurement and Control*, pp. 303-309.

**[Yuan,88]** Yuan, Joseph S.-C., "Closed-Loop Manipulator Control Using Quaternion," *IEEE Transactions of Robotics and Automation*, Vol. 4, No. 4, Aug. 1988, pp. 434-440.